American Journal of Materials Science 2015, 5(3A): 1-7
DOI: 10.5923/s.materials.201502.01

Dielectric Surface Currents and Dielectric Constant Measurements of Pure and Multi-walled Carbon Nanotubes (MWCNT) Doped Polyvinyl Alcohol Thin Films

Matthew Edwards[1,2,*], Padmaja Guggilla[1,*], Afef Janen[1], Jemilia Polius[1], Stephen Egarievwe[3], Michael Curley[1]

[1]Department of Physics, Chemistry and Mathematics, Alabama A&M University, Normal, USA
[2]Institute of Higher Science Education Advancements and Research (IHSEAAR), New Market, USA
[3]Department of Electrical Engineering and Computer Science, Alabama A&M University, Normal, USA

Abstract The objectives of this research were to characterize dielectric surface currents under the influence of temperature, and low electrical voltages (low electric fields) and the dielectric constant, and dielectric loss during variations in temperature and low frequencies of three different materials, namely, commercial paper, pure polyvinyl alcohol (PVA) thin films, and multi-walled carbon nanotubes (MWCNT) doped PVA thin films. It was recognized that nano-dopants, microscopic structure, and environmental conditions contributed to unique physical properties of these material systems. Specifically, electric surface current densities J_s were measured on the surface of pure and MWCNT doped PVA thin films, and were found, differently than initially surmised, to be produced through ohmic conduction or space-charge conduction, as the two are indistinguishable at low voltages yielding a surface-limited conduction phenomenon only. The dielectric constant measurements were observed to compare well with the fundamentals of the Cole-Cole equations, and dielectric losses resulted from electromagnetic energy loss through phase differences between low-frequency input signals and time varying polarization. In addition, both the dielectric constant and the dielectric loss were observed to be highest for MWCNT doped PVA compared to pure PVA and commercial paper, and significant variations occurred with frequency and temperature for all samples. While both surface-limited and electrode-limited electron conductions may occur when dielectrics and metallic electrodes are interfaced, none of the latter outcomes were observed in this research.

Keywords Dielectric Surface Currents, MWCNT Doped PVA Thin Films, Dielectric Constant, Dielectric Loss, Ohmic Conduction, Space-charge Conduction

1. Introduction

While it may appear counterintuitive to investigate dielectric surface currents, dielectric constants, and the electric losses of organic thin films in the same research, we have found it advantageous to do so in this study. Our rationale originates from the fact that a functional understanding of both conduction and insulation properties is needed for the efficient use of dielectric materials in electronic devices, such as in printed circuit boards (PCBs), charge-coupling devices (CCDs), and digital imagers [1-3]. These systems require electric currents to exist only along specific conduction paths, while traveling between electrical components, and not to occur in an undesignated manner. In this regard, as device miniaturization occurs and switching speeds increase, the onset of crosstalk currents or unaccounted stray moving charges hasten to compromise electric circuits [4]. Thus, it is critically important to eliminate the causes of electronic device failure before it occurs and be able to predict the likelihood of failure by understanding the crosstalk phenomenon and other stray current issues prior to using a material, whether or not it exists in the form of a simple conduct, a dielectric, or a material having both behaviors. Otherwise, untimely failure or faulty performance is the likely outcome.

For this research while being cognizant of the many anomalies existing in dielectric material measurements via the application of parallel plate capacitance [5], we have, nevertheless, measured the low-frequency dielectric constant and the dielectric loss. The governing equations are:

* Corresponding author:
mtthwedwards7@gmail.com (Matthew Edwards)
Padmaja.guggilla@aamu.edu (Padmaja Guggilla)
Published online at http://journal.sapub.org/materials

$$\varepsilon' = \frac{C_p d}{\varepsilon_0 A} \quad (1)$$

$$\varepsilon'' = \varepsilon' \tan\delta \quad (2)$$

where ε' is the dielectric constant, C_p is the parallel plate capacitance, tanδ is the dielectric loss tangent, A is the electrode area, d is the thickness of the sample, ε" is the dielectric loss, and $\varepsilon_0 = 8.854\times10^{-12}$ F/m is the vacuum permittivity. The dielectric constants were determined from equation (1) and the dielectric losses from equation (2). All measured values have been reported in the below Results and Discussion section.

Regarding the surface current conduction nature of dielectrics, it has been suggested that low-level currents may exist in ordinary dielectrics resulting from two broad categories. Bulk-limited conduction mechanisms, resulting from impurities and defects in the dielectric, are the first kind of conduction, and electrode-limited conduction mechanisms, occurring from electrode origination of charge carriers, are the second [6]. Several current conduction processes have been determined to depend on the electrical properties at the electrodes-dielectric interface, and others depend only on bulk-surface-limited conduction mechanisms. Complementing the Drude model of simple conductors, which has a plasma resonance frequency, table 1 gives some of the important conduction mechanisms in dielectrics [6, 7]. The methods to distinguish between these conduction mechanisms are essential since several conduction mechanisms may contribute to the total conduction current through the dielectric or on its surface. Moreover, measuring the temperature-dependent conduction currents or the electrical voltage dependence may provide a useful method to understand or differentiate the constituted currents, since many conduction mechanisms depend on temperature and voltages in different ways. In addition, electrode-limited conduction mechanisms are implemented only at high voltages, as the electrons must be ejected from the metallic surface before conduction can occur [6].

Table 1. Important Conduction Mechanisms In/On Dielectrics

Electrode-Limited Conduction Mechanisms	Bulk-Surface-Limited Conduction Mechanisms
1. Schottky emission	1. Poole-Frenkele emission
2. Fowler-Nordheim tunneling	2. Hopping conduction
3. Direct tunneling	3. Ohmic conduction
4. Thermionic-field emission	4. Space-charge-limited conduction
	5. Ionic conduction
	6. Grain-boundary-limited conduction

Source: Reference [6].

Perfect dielectrics, with large band gaps, are known to have no conduction electrons at zero degrees Kelvin, as the valence band is completely filled and the conduction band empty at this temperature. Moreover, above zero Kelvins, due to thermal fluctuations, some electrons do transition to the conduction band and manifest as conduction electrons, and owing to the presence of impurities and defects in ordinary dielectric materials, additional electrons exist in the conduction band. It is the presence of these conduction electrons that lead to surface current conduction, and we have sought to ascertain the cause of the observed surface current measurements in this study. To that extent, we have measured dielectric surface currents in the range of 10^{-9} to 10^{-6} amps for low voltages, resulting from Ohmic conduction on the surfaces of dielectrics or the equivalent space-charge conduction. For thin films, the Ohmic conduction mechanism [6] is described by equation (3)

$$J_s = \sigma_s E = q\mu E N_c \exp\left[-\frac{(E_c - E_F)}{kT}\right] \quad (3)$$

where J_s is the surface current density (measured in amp/m), σ_s is the electrical conductivity, E is the electric field, q is the electron charge, μ is the electron mobility, N_c is the effective density of quantum states of the conduction band, E_c is the energy in the conduction band, E_F is the Fermi energy, k is the Boltzmann constant, and T is the temperature. Equation (3) depicts the linearity between surface current density J_s and the electric field E. Similarly, in a flat-electrode configuration at low voltages, space-charge conduction [6, 7] is described by

$$J = qn_0\mu\frac{V}{d} \quad (4)$$

where n_0 is the concentration of free charge carriers, d is the constant distance between the electrodes, and the other quantities are as defined above. Equations (3) and (4) show clearly the equivalence of Ohmic conduction and space-charge conduction, at low voltages, for surface-limited conduction mechanisms. In addition, even a perfect dielectric, when connected to metallic electrodes, can yield surface currents independent of surface-limited conduction when strong electric fields ($E > 10^6$ V/m) exist, yielding current occurring from electrode-limited mechanisms, such as Schottky emission or direct tunneling. Moreover, the opportunity exists, with high electric fields, to have conduction occurring simultaneously from both surface-limited conduction and electrode-limited conduction. In this study, we have observed only surface-limited conduction with a low voltage applied across a concentric circular space gap of d = 1/8 inch (3.20 mm).

On applying 90 - 500 volts to the samples, we measured, for pure PVA, MWCNT doped PVA, and for commercial paper, surface currents in the range from 10^{-9} – 10^{-6} amp. Currents in this lower voltage range were of the Ohmic kind, while currents resulting from higher voltages suggest charge movement from not only Ohmic conduction or space-charge but possibly other surface-volume-limited behaviors, such as hopping conduction and from electrode-limited conduction as well.

While many studies over the past century have been

conducted on bulk conduction [8], only recently has surface current conduction began to be considered, partly driven by the consequences of miniaturized of printed circuit boards (PCBs), and charge-coupling devices (CCDs), where crosstalk possibilities are becoming inevitable. Thus, knowing volume current conduction was often sufficient to meet the application of materials in previous applications, the focus has changed to include electrical surface conduction, as well [9-11]. To that extent, we have observed a surface current density J_s when both anode and cathode are placed on the same side of a material, contrasted to bulk currents, where the electrodes are on opposite ends of the sample. In comparison, bulk current density exists through a perpendicular area, measured in amp/m^2, while surface current density exists through a perpendicular length expressed in amp/m, and although the two are conceptually different, each as a physical quantity pertaining to conduction is worthy of being determined.

In this regard, we previously measured surface resistivity as function of temperature of pure and MWCNT doped PVA thin films and of Ag nano-particles doped PVA [12-15]. Samples of commercial paper were measured as well since paper is often used as insulation for circuit components. Our calculated surface resistivity values, in the temperature range from 20 to 40℃, yielded a pattern of initial decreasing resistivity to a minimum value as the temperature increased, but began to rise and to continue as such up to the experimental limit of our test fixture [14] near 40℃. Moreover, MWCNT and Ag nano-particle doped samples showed a more pronounced variation in the same temperature range than did the pure samples [16, 17].

However meaningful these results were to understanding dielectric surface conduction, they were unable to explain fully the surface current conduction phenomenon that may exist on the surface of dielectric materials. To consider dielectric surface current conduction further, we have measured dielectric surface current density J_s of pure and doped MWCNT PVA thin films samples resulting from low-level applied voltages, ranging from 0 to 500 volts. The pure PVA and the commercial paper samples results, differently than initially surmised, significantly yielded data points that matched remarkably well the simple Ohmic conduction. In addition, the doped PVA samples matched the Ohmic conduction at lower voltages but deviated at higher voltages, suggesting possible contribution from other surface-limited conduction mechanisms, such as hopping conduction.

Additionally, we have measured the dielectric constant and dielectric loss of our samples. The observed results are depicted in section 3 for the pure, and MWCNT doped samples and the commercial paper.

2. Experimental and Methods

Dielectric surface currents, as a function of temperature and low applied voltages, have been measured using the combined Keithley Model 6517 Electrometer and Keithley Model 8009 resistivity test fixture with the Amprobe wireless thermometer coupled to a J-type thermocouple as shown in Figure 2a. This figure displays all critical components of the setup. Humidity, another important external factor in surface conduction measurements, was monitored with a commercial grade humidifier.

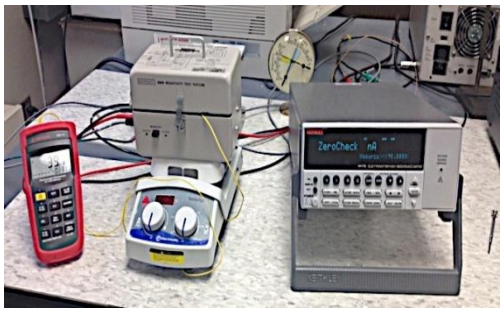

Figure 2a. Experimental Setup #1, Surface Current Measurements

In this research, we specified humidity as normally low, normally medium, or normally high. All of our reported measurements were made at normal medium humidity at approximately 70%.

Figure 2b, below, gives the electrodes configuration of the test fixture, depicting the surface current measurement method, with a guarded electrode at the top, and two circular electrodes at the bottom with the sample sandwiched between. The gap spacing d between the electrodes is 1/8 inch (3.20 mm).

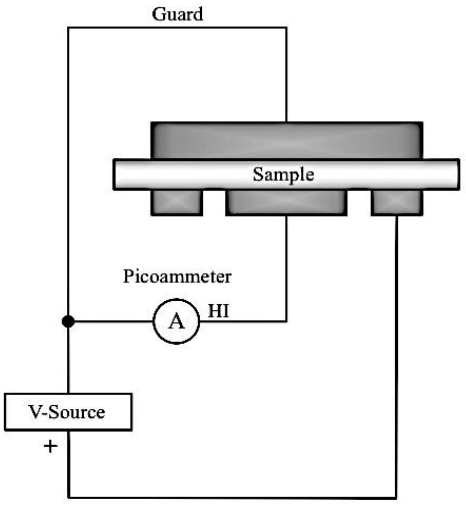

Figure 2b. Illustration of Current Path with the Sample in Position and Concentric-Circles Bottom Electrodes and the single top Electrode

The mathematical equations of the electrode configuration [Keith's manual] yield the relationship between voltage V and inner R_1 (= 25.4mm) and outer radius R_2 (=28.6mm) as

$$V = \int_{R_1}^{R_2} E dr = \int_{R_1}^{R_2} \frac{\rho_s I_s}{2\pi r} dr = \frac{\rho_s I_s}{2\pi} \ln\left(\frac{R_2}{R_1}\right) = \frac{\rho_s I_s}{2\pi} \ln\left(\frac{R_1 + d}{R_1}\right) = \frac{\rho_s I_s}{2\pi} \ln\left(1 + \frac{d}{R_1}\right) = \frac{\rho_s I_s}{2\pi} \ln(1 + b) \quad (5)$$

where ρ_s is the surface density, I_s is the surface current.

$$R_2 = R_1 + d, and\, b = d / R_1.$$

Since b << 1 [18]

$$\ln(1+b) = b - \frac{b^2}{2} + \frac{b^3}{3} - \frac{b^4}{4} + \cdots \approx b \qquad (6)$$

$$when -1 < b \le 1 \;\; and \;\; b = 1/8 << 1$$

$$V \approx \frac{\rho_s I_s b}{2\pi} = \frac{\rho_s I_s}{2\pi}\frac{d}{R_1} = E(r = R_1)d \qquad (7)$$

$$where\, E(r = R_1)\, is\, the\, electric\;\; field\, at\, the\, inner\, radius\;\; R_1$$

Also, the surface current density is needed that is given as

$$J_s = \frac{I_s}{2\pi R_1}. \qquad (8)$$

Equation (7) yields the calculated electric field E at the inner radius electrode when known voltage V is applied, and d = 3.20 mm is the constant distance between the electrodes, allowing equation (8) to give the surface current density at the inner radius R_1.

Figure 2c shows the commercial paper thin film sample, the pure PVA, and the MWCNT PVA sample as prepared from the convention evaporation technique to make PVA thin films [19].

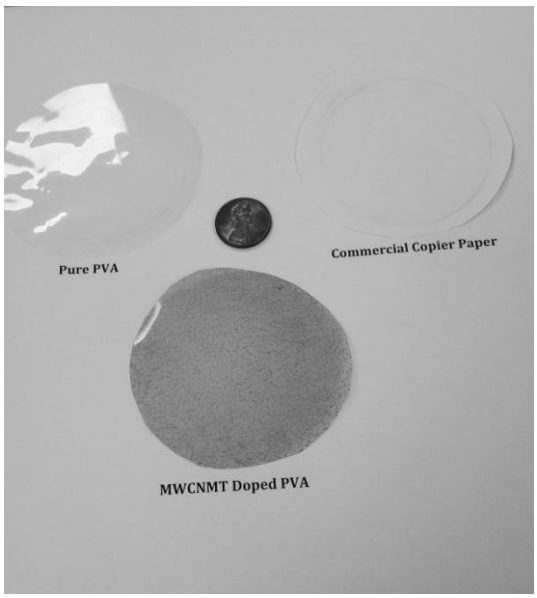

Figure 2c. Pure and Doped PVA Films and Commercial Paper

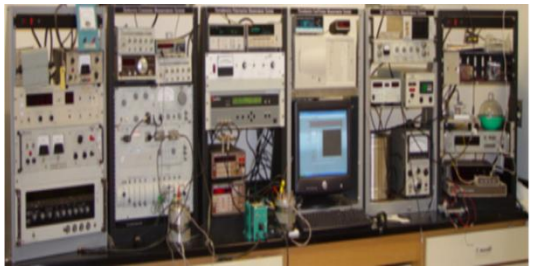

Figure 2d. Experimental Setup #2, Dielectric Constant, Dielectric Loss, and Other Electrical Measurements

Figure 2d gives the experimental setup that was used to measure the dielectric constant and dielectric loss as a function of temperature and frequencies. See reference [15] for details of its components.

3. Results and Discussion

3.1. Dielectric Surface Currents

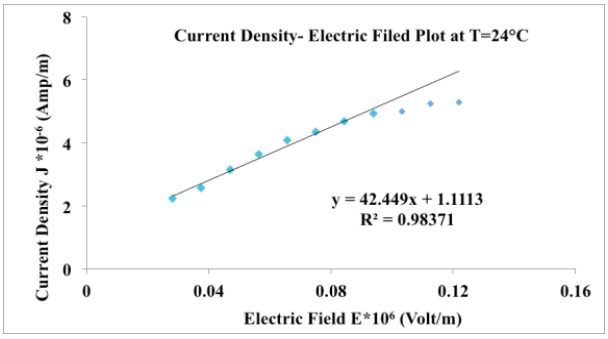

Figure 3a. Doped Sample: Current Density J_s Vs. electric field, E(r=R_1)

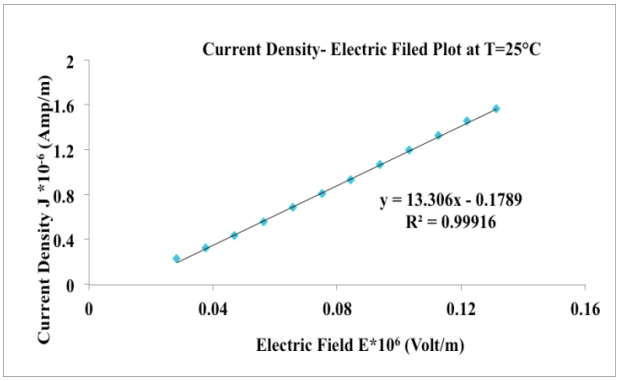

Figure 3b. Undoped Sample: Current Density J_s Vs. electric field, E(r=R_1)

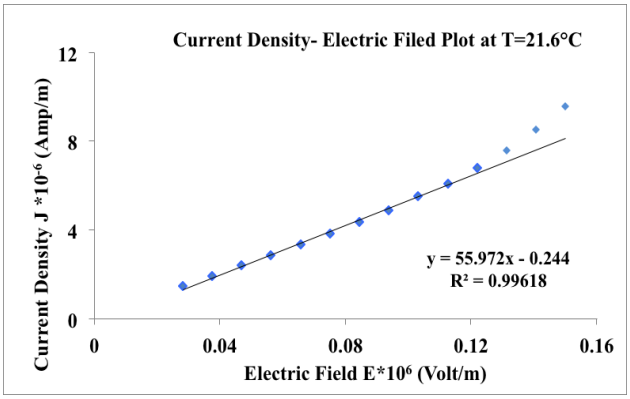

Figure 3c. Commercial Copier Paper: Current Density J_s Vs. Electric Field, E(r=R_1)

Figure 3a gives the dielectric surface current density J_s as a function of electric field at the inner radius E(r=R_1) for the MWCNT doped PVA thin film at 24℃. The graph is linear over the span of the electric field supporting the ohmic conduction mechanism. Similarly, Figures 3b and 3c provide comparable results for the pure PVA film at 25℃ and the commercial paper at 21℃, respectively. In comparison, the

surface current density MWCNT doped PVA is larger over the range of electric field than for commercial paper film or the pure PVA, indicating a greater number of charge carriers in the conduction band of the doped material. The voltage range was from 0 to 420 volts for all samples used, and while Figure 3a – 3c, visually depict straight-line results, linear regression fitting further confirms the observed outcomes, especially at low electric fields.

3.2. Dielectric Constant and Dielectric Loss

Chemical and mechanical stability properties of materials with low processing cost have extensive applications in the electronic industry such as the multilayer ceramic substrate for electric devices in integrated circuits, magnetic disk substrate for high storage capacity, and sensor technology. Figures 3d and 3e show the variations of the dielectric constant and dielectric loss versus frequency at different test temperatures.

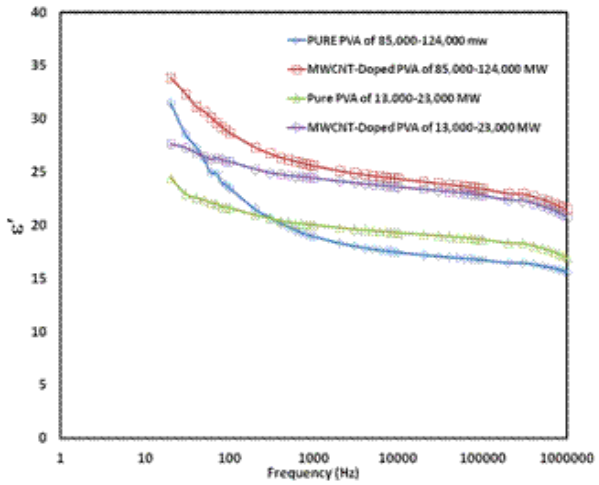

Figure 3d. Variations of the Dielectric Constant Vs Frequency at Different Temperatures

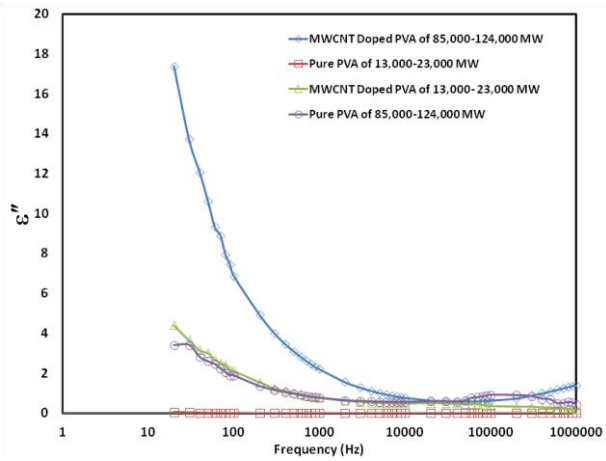

Figure 3e. Variations of the Dielectric Loss Vs Frequency at Different Temperatures

From both figures, it is evident that the dielectric constant and the dielectric loss decreased sharply with increasing frequency when measuring frequency lower than 1 KHz at all test temperatures, but decreased slowly when frequency ranged from 1 KHz to 1 MHz. The reduction of the dielectric constant with increasing frequency may be attributed to that the ionic and orientation polarization gradually becomes weakened or disappeared with increasing frequency, and the decrease of the dielectric loss with increasing frequency was mainly due to ions migration polarization loss, and the electronic polarization loss may exist at low frequency, while at higher frequency variation in charge or ion vibrations may be the only source of the dielectric loss [20-25]. The MWCNT doped sample showed the highest dielectric constant and dielectric loss compared to other samples, which may be due to the amount of increased interstitial dopant in the sample. The increase of the ε′ was larger for the MWCNT doped PVA compared to pure PVA.

Figures 3f and 3g show that the dielectric constant and the dielectric loss are increasing with an increase in temperature.

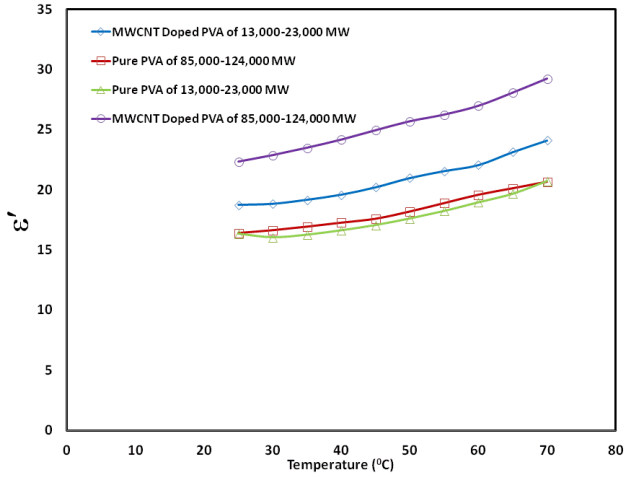

Figure 3f. Variations of the Dielectric Constant Vs Temperature at Different Frequencies

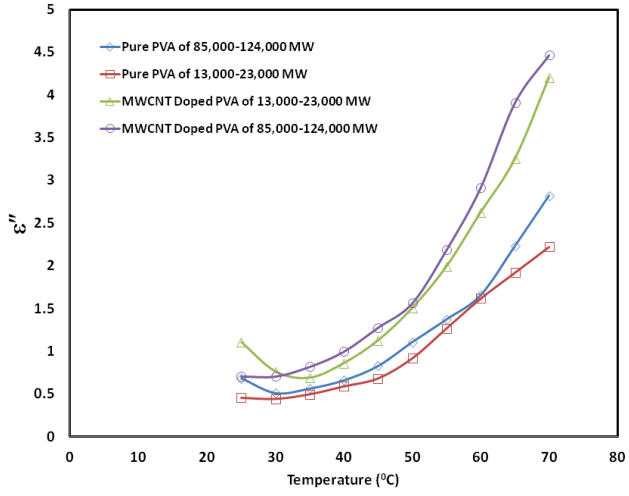

Figure 3g. Variations of the Dielectric Loss Vs Temperature at Different Frequencies

The values of the dielectric constant and the dielectric loss were only in the range of 15 - 35 and 0.5 - 5 respectively, which is close to the reported values. When the temperature

increased from 40℃ to 70℃, the value of the dielectric constant increased in the range of 20 - 35 and the dielectric loss increased in the range of 1 - 5. Thus, the temperature has a significant influence on the dielectric properties of these materials. The increase of the dielectric constant with temperature was attributed to the increase of electronic, ionic, and orientation polarizability with increasing temperature, and the increase of the dielectric loss with increasing temperature was due to a rapid increase of the relaxation loss and the conduction loss with increasing temperature. The temperature and frequency have significant influence on the dielectric properties of these samples. The dielectric constant and dielectric loss of composite materials decreased with increasing frequencies, and the dielectric constant and dielectric loss increased with temperature. Based on preliminary results, it is evident that all the samples are functional and variation in molecular mass PVA powder yielded changes to the dielectric constant and the dielectric loss. The addition of MWCNT dopants enhanced the dielectric properties by increasing both the dielectric constant and the dielectric loss, which can be attributed to the amount of the interstitial dopant being deposited in the thin films.

Samples doped by SWCNT show the highest dielectric constant and dielectric loss compared to the other samples due to the amount of the interstitial dopant.

4. Conclusions

While the ohmic conduction or space-charge conduction emerged as the dominate mechanism in contributing conduction electrons in surface-limited conduction behavior, in all samples, of pure PVA, MWCNT doped PVA, and commercial paper, other surface-limited mechanisms were contributing at higher electric fields for MWCNT doped PVA and commercial copier paper. No electrode-limited conduction processes were present in our samples. Additionally, MWCNT doped PVA samples showed the highest dielectric constant and dielectric loss compared to other samples considered. Moreover, preliminary results indicate that all the samples were functional and variation in molecular mass PVA powder yielded changes to the dielectric constant and the dielectric loss. More studies will be necessary to deduce the additional cause(s) of surface current conduction other than ohmic or space-charge conduction, of the observed increases in the dielectric constant and dielectric loss values due to MWCNT dopants in PVA thin films, and of the observed variations of the dielectric constants with changes in the molecular mass of the PVA powder.

ACKNOWLEDGEMENTS

The authors would like to thank DHS grant 2012-DN-077-ARI065-04, DHS-SLA Award Grant # 2010-ST-062-000034, the Evans Allen grant of USDA, HBCU-UP grant and APEX grant of NSF for partial funding of this research, and to Chairperson Dr. Mohan Aggarwal for continued support of our research agenda, and Dr. Jacob Oluwoye for helpful discussions and motivational support.

REFERENCES

[1] W. A. Maryniak, T. Uehara, and M. A. Noras, "Surface resistivity and surface resistance measurements using a concentric ring probe technique," Trek Application Note, 0623/MAN Rev. 1b (1005), 2003.

[2] F. C. Chiu and C. M. Lai, "Optical and electrical characterization of cerium oxide thin films," Journal of Physics D, vol. 43, no. 7, Article ID 075104, 5 pages, 2010.

[3] D. J. Griffiths, *Introduction to Electrodynamics*, Prentice Hall, 3th ed., 1999.

[4] L. N. Charyulu, Annapurna Das, and Sisir K. Das, "Analysis and Measurement of crosstalk in printed circuit board due to RF and transient pulses," in Proc. INCEMIC, 2003, paper, pp. 257-260.

[5] J. F. Nye, *Physical Properties of Crystals,* Oxford Science Publications, 1985.

[6] Fu-Chien Chiu, "A review on conduction mechanisms in dielectric films," Advances in Materials Science and Engineering, Hindawi Publishing Corporation, Article ID 578168, pp. 1-18, 2014.

[7] H. Akinaga and H. Shima, "Resistive random access memory (ReRAM) based on metal oxides," Proceedings of the IEEE, vol. 98, no. 12, pp. 2237-2251, 2010.

[8] Q. Li, Q. Z. Xue, X. L. Gao, and Q. B. Zheng, "Temperature dependence of the electrical properties of the carbon nanotube/polymer composites," eXPRESS Polymer Letters, 3(12), pp. 769-777, 2009.

[9] C. K. Wong, and F. G. Shin, "Electrical conductivity enhanced dielectric and piezoelectric properties of ferroelectric 0-3 composites," J. Appl. Phys., 97, 064111, 2005.

[10] J. Borch, M. Lyne, R. Mark, and C. Habeger Jr., *Handbook of Physical testing of Paper*, CRC Press, vol. 2(2), 2010.

[11] C. Kittel, *Introduction to Solid State Physics*, John Wiley and Sons, Hoboken. 8th ed., 2005.

[12] Matthew Edwards, Padmaja Guggilla, John C. Corda, and Stephen Egarievwe, "Measurement of the dielectric, conductance, and pyroelectric properties of MWCNT:PVDF nanocomposite thin films for application in infrared technologies," SPIE Vol. 8868, no. 11, 2013.

[13] Matthew Edwards, Stephen Egarievwe, Tatiana Kukhtarev, and Jemilia Polius, "Surface resistivity temperature dependence measures of commercial, multiwall carbon nanotubes (MWCNT), or silver nano-particle doped polyvinylidene difluoride (PVDF) and polyvinyl alcohol (PVA) films," SPIE Vol. 9220, 922009, 2014.

[14] Matthew Edwards, Stephen Egarievwe, Afef Janen, Tatiana Kukhtarev, Jemilia Polius, and John Corda, "Temperature

Dependent Surface Resistivity Measures Of Commercial, Multiwall Carbon Nanotubes (MWCNT), and Silver Nano-Particle Doped Polyvinyl Alcohol (PVA) Films," Materials Sciences and Application Journal, Vol. 5, pp. 915-922, 2014.

[15] A. K. Batra, M. E. Edwards, P. Guggilla, M. D. Aggarwal, and R. B. Lal, "Pyroelectric Properties of PVDF: MWCNT Nanocomposite Film for Uncooled Infrared Detectors and Medical Applications", Integrated Ferroelectrics, Vol. 158, Iss.1, 2014.

[16] E. Y. Malikov, M. B. Muradov, O. H. Akperov, G. M. Eyvazova, R. Puskas, L. Madarasz, A. Kukovecz, and Z. Konya, "Synthesis and characterization of polyvinyl alcohol based multiwalled carbon nanotube nanocomposites," Physica E., 61, pp. 129-134, 2014.

[17] Jacob N. Israelachili, *Intermolecular and Surface Forces, with applications to colloidal and biological systems*, Academic Press, 1985.

[18] Murray R. Spiegel and John Liu, *Mathematical Handbook of Formulas and tables*, 2nd. Ed., Schaum's Outlines, McGraw-Hill, New York, NY, 1999.

[19] Chem-Fax, Flinn Scientific, INC., Publication No. 608.00, (2010).

[20] M. M. Elkholy and L. M. Sharaf, "Effect of P_2O_5 on Microstructure and Properties of Calcium Aluminoborosilicate Glasses," Mater. Chem. Phys. vol. 65, no. 192, 2000.

[21] Sreelalitha Kramadhati and K. Thyagarajan "Optical Properties of Pure and Doped (KNO_3 & $MgCl_2$) Polyvinyl Alcohol Polymer Thin Films," International Journal of Engineering Research and Development, vol. 6, issue 8, pp. 15-18, 2013.

[22] K. Lang, S. Sourirajan, T. Matsuura, and G. Chowdhury, "A study on the preparation of polyvinyl alcohol thin-film composite membranes and reverse osmosis testing," Desalination, vol. 104, issue 3, pp 185-196, May 1996.

[23] John Reitz, Frederick Milford and Robert Christy, *Foundations of Electromagnetic Theory*, 3rd Edition Addison-Wesley Publishers, 1980.

[24] Vikram S. Yadav, Devendra K. Sahu, Yashpal Singh, and D.C. Dhubkarya, "The Effect of Frequency and Temperature in Dielectric Properties of Pure Poly Vinylidene Fluoride (PVDF) Thin Films," Proceedings of the International Multi-Conference of Engineers and Computer Scientists 2010 Vol III, IMECS 2010, March 17-19, 2010, Hong Kong.

[25] Matthew Edwards, Padmaja Guggilla, John C. Corda, and Stephen Egarievwe, "Measurement of the dielectric, conductance, and pyroelectric properties of MWCNT:PVDF nanocomposite thin films for application in infrared technologies", SPIE Vol. 8868, no. 11, 2013.